

# Therapeutic Efficacy of Replication-Competent Retrovirus Vector–Mediated Suicide Gene Therapy in a Multifocal Colorectal Cancer Metastasis Model

Kei Hiraoka,<sup>1</sup> Takahiro Kimura,<sup>1</sup> Christopher R. Logg,<sup>1</sup> Chien-Kuo Tai,<sup>1</sup> Kazunori Haga,<sup>1</sup> Gregory W. Lawson,<sup>2</sup> and Noriyuki Kasahara<sup>1</sup>

<sup>1</sup>Department of Medicine and <sup>2</sup>Division of Laboratory Animal Medicine, University of California Los Angeles, Los Angeles, California

## Abstract

**Replication-competent retrovirus (RCR) vectors are intrinsically incapable of infecting quiescent cells and have been shown to achieve highly efficient and tumor-restricted replicative spread and gene transfer *in vivo* after direct intratumoral injection in a variety of primary cancer models. However, *i.v.* delivery of RCR vectors expressing therapeutic genes has never previously been tested, particularly in an immunocompetent tumor model. Therefore, in the present study, we sought to test the therapeutic effect of an RCR vector (ACE-CD) carrying the yeast cytosine deaminase (CD) gene, which converts the nontoxic prodrug 5-fluorocytosine (5FC) into the chemotoxin 5-fluorouracil, after delivery by infusion into the locoregional circulation in a multifocal hepatic metastasis model of colon cancer. After confirmation of suicide gene cytotoxicity *in vitro*, multifocal hepatic tumors were established in syngeneic mice with murine CT26 colorectal cancer cells expressing firefly luciferase (CT26.FLuc), and the ACE-CD vector was infused via intrasplenic injection into the portal circulation. Fourteen days after locoregional infusion, systemic administration of 5FC resulted in significant inhibition of bioluminescent signals in mice whose tumors had been infected with RCR but not in control mice. Notably, there was no detectable RCR vector spread to normal liver or bone marrow by quantitative PCR analysis. Our results thus show that locoregional delivery of a suicide gene by RCR vectors infused into the portal circulation results in progressive transduction of multiple tumor foci in the liver, without evidence of spread to adjacent normal parenchyma or extrahepatic tissues, and can achieve significant tumor growth inhibition. [Cancer Res 2007;67(11):5345–53]**

## Introduction

Despite all efforts, colorectal cancer remains the third most common cancer in both men and women in the United States, accounting for ~150,000 new cases annually (1). The liver is the most common site of metastasis, with up to 70% of colorectal cancer patients eventually developing liver metastases, which are still confined to the liver at the time of metastatic diagnosis in 30% to 40% of these patients. However, only one-fourth of patients with metastases confined to the liver are surgical candidates due to tumor

size, distribution, or accessibility (2–4). The mainstay of nonsurgical treatment for advanced colorectal cancer has been 5-fluorouracil (FU), and current chemotherapeutic regimens generally consist of FU/leucovorin (folate) combined with newer agents, such as CPT-11 (5–7) or oxaliplatin (8, 9). Nonetheless, whereas early-stage, organ-confined disease is associated with a good prognosis for advanced colorectal cancer defined by the presence of metastatic disease, the 5-year survival rate is still extremely poor. Thus, the development of new therapeutic approaches that can affect liver metastasis represents one of the most important factors for improving the prognosis of patients with advanced colon cancer.

A variety of gene therapy approaches for advanced colorectal cancer have been investigated, in particular suicide gene therapy which results in the intracellular conversion of nontoxic prodrugs into potent chemotoxins directly within the cancer cell (10–13); but when translated to clinical trials, many such approaches have failed due to the inability to achieve effective gene delivery *in vivo* to multiple metastatic tumor foci, immunologic responses that neutralize the vector, and short-term duration of any therapeutic effects (14). More effective gene delivery could be achieved by the use of tumor-selective replication-competent viruses, as each transduced tumor cell would itself become a virus producer cell, thereby sustaining further transduction beyond the initial inoculum. Indeed, the use of replication-competent viruses as oncolytic agents shows great promise as a reemerging field of experimental therapeutics (15, 16), and recent studies using an oncolytic adenovirus have shown survival benefit in clinical trials for advanced colorectal cancer (17, 18). However, there remains a need for more potent agents that will achieve more durable effects and can be readministered or will persist in residual tumor tissues.

Here we have tested, in an advanced colorectal cancer model, a replication-competent retrovirus (RCR) vector based on amphotropic murine leukemia virus (MLV), which we have previously shown to be capable of achieving highly efficient replicative spread and gene delivery throughout solid tumors *in vivo* (19–22). Replication of the RCR is intrinsically selective for tumors, as MLV can infect only actively dividing cells (23). Furthermore, unlike other replicating viruses that have previously been tested in metastatic liver tumor models, such as adenovirus (24, 25), herpes virus (26–28), or vaccinia virus (29, 30), retrovirus replication is not oncolytic in itself and results in permanent integration of the virus into the host cell genome; but this unique feature allows RCR vectors to achieve more persistent replication and longer duration of transgene expression in solid tumors, resulting in significant therapeutic benefit in intracranial glioma models (31, 32).

Recently, we have shown that RCR vectors can achieve efficient transduction of multifocal murine CT26 colorectal cancer metastases in the liver even after locoregional delivery through the portal circulation in an immunocompetent syngeneic host. A single

**Requests for reprints:** Noriyuki Kasahara, University of California at Los Angeles Geffen School of Medicine, MRL-1551, 675 Charles E. Young Drive South, Los Angeles, CA 90095. Phone: 310-825-7112; Fax: 310-825-5204; E-mail: nkasahara@mednet.ucla.edu.

©2007 American Association for Cancer Research.  
doi:10.1158/0008-5472.CAN-06-4673

infusion of RCR vectors resulted in replicative spread and selective transduction with a green fluorescent protein (GFP) marker gene in multiple orthotopic tumors in the liver *in vivo*, sparing normal hepatocytes and without dissemination to extrahepatic normal tissues (33).

In the present study, we used both s.c. tumor and multifocal liver metastasis models of CT26 colorectal cancer to test the therapeutic effectiveness of RCR vectors expressing the yeast cytosine deaminase (CD) suicide gene, which can convert the nontoxic antifungal drug 5-fluorocytosine (5FC) into FU directly within the infected tumor cell (12, 13, 34, 35). The syngeneic liver metastasis model, in particular, represents one of the most stringent challenges to experimental therapies due to its extremely aggressive nature and multiple tumor foci in the context of an immunocompetent host. In previous studies using this model, continuous infusion of FU itself at the maximum tolerated dose showed no therapeutic benefit (36). Our results indicate that RCR vector-mediated suicide gene therapy delivered by locoregional infusion can achieve significant growth inhibition in this orthotopic model, indicating the potential utility of this strategy for advanced colorectal cancer.

## Materials and Methods

**Cell lines.** Transformed human embryonic kidney cell line 293T was maintained in DMEM. BALB/c-derived murine colon adenocarcinoma cell line CT26 was maintained in RPMI 1640. Human colon adenocarcinoma cell lines WiDr and LoVo were maintained in MEM medium and Ham's F12K medium, respectively. Each medium was supplemented with 10% fetal bovine serum and 1% penicillin-streptomycin. All the cell lines were obtained from American Type Culture Collection and maintained in a humidified atmosphere with 5% CO<sub>2</sub>.

**Viral vector plasmid and virus production.** The plasmids pACE-GFP and pACE-CD have been described previously (20, 32); each contains a full-length replication-competent amphotropic MLV provirus with an additional internal ribosome entry site (IRES)-GFP or IRES-CD cassette, respectively (Figs. 1A and 3A). For virus production, 293T cells were transiently transfected with pACE-GFP or pACE-CD using Fugene-6 (Roche Diagnostics Corp.), replenished with serum-free medium, and 48 h later the supernatant medium was harvested, filtered, and stored frozen at -80°C. For production of replication-defective retrovirus vector expressing GFP (MLV-GFP), plasmids pCGP (MuLV *gag-pol*), pCAE (amphotropic 4070A *env*), and vector pMLV-GFP were cotransfected as previously described (37).

Polybrene (4 µg/mL; Sigma) was added to all cultures before infection. Viral titers were determined in the presence of 50 µmol/L 3'-azide-3'

deoxythymidine (AZT; Sigma) to prevent replication. After 48 h, GFP expression was analyzed with a Coulter EPICS Flow Cytometer (Beckman-Coulter). Viral titers in transducing units (TU) per milliliter were calculated as described previously (32).

The self-inactivating (SIN) lentiviral vector in this study was derived from the pRRL-sin-cPPT-hCMV-MCS-pre vector as described previously (38). Firefly luciferase cDNA was inserted in the multiple cloning site of the vector. Virus production was done by transient cotransfection of 293T cells as described (38), and titers were determined by measuring viral p24 antigen concentration by ELISA (Coulter Immunotech).

**Replication kinetics of RCR *in vitro*.** For analysis of replication kinetics *in vitro*, virus vector stock at multiplicity of infection (MOI) = 0.01 was used for infection of WiDr or LoVo cells at 20% confluency or at MOI = 0.05 for CT26 cells at 20% confluency. At serial time points, the cells were trypsinized, one-fourth was replated, and the remainder was analyzed for GFP expression by flow cytometry. As nonreplicating controls, replication-defective MLV-GFP vector was used instead of ACE-GFP or 50 µmol/L AZT was added into the cultured medium of ACE-GFP infected cells to prevent virus spread. A stably transduced cell population (CT26.GFP) that reached almost 100% transduction with ACE-GFP was maintained for further experiments.

**Replication kinetics in s.c. tumor models.** Six- to eight-week-old female BALB/c mice (Charles River Laboratories Inc.) were bred and maintained under specific pathogen-free conditions, and all studies conducted under protocols approved by the University of California at Los Angeles Animal Research Committee.

For s.c. tumor models, CT26.GFP cells were mixed with uninfected parental CT26 cells at various ratios (0.5%, 2%, and 100%), and these CT26 cell mixtures ( $5 \times 10^4$  cells) in 100 µL PBS were s.c. injected into the right dorsal flanks of BALB/c mice. Two weeks later, s.c. tumors were excised, minced, and separated from extraneous tissue under sterile conditions, digested with collagenase/dispase (1 mg/mL; Roche Diagnostics) for 2 h at 37°C. Dissociated cells were passed through a 100-µm cell strainer, pelleted by low speed centrifugation, and resuspended in PBS. Half of the cells were analyzed by flow cytometry for GFP expression, and the remainder placed in explant culture. As a control group, half of the mice received AZT (0.4 mg/mL) in the drinking water throughout the experiment, starting from 1 day before tumor inoculation.

**Expression of yeast CD in CT26 cells infected with ACE-CD.** CT26 cells were infected with ACE-CD at MOI of 0.1 in parallel with ACE-GFP under identical conditions, which showed >95% transduction by day 18. To confirm expression of yeast CD protein in this stably transduced cell population (CT26.CD), Western blot analysis was done for yeast CD. Untransduced parental CT26 cells, CT26.GFP cells, and CT26.CD cells were collected, washed twice with PBS, and resuspended in ice-cold cell lysis buffer composed of 50 mmol/L Tris-HCl (pH 7.5), 1 mmol/L EDTA, 150 mmol/L NaCl, 0.1% SDS, 0.5% deoxycholic acid, and 1% Igepal CA-630 with

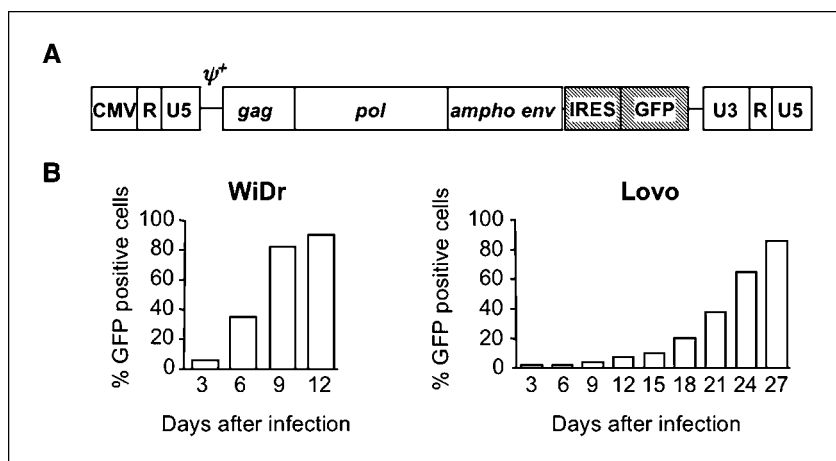


**Figure 1.** A, design of RCR vector ACE-GFP. This vector contains a full-length replication-competent MLV proviral sequence, in which an IRES-GFP cassette has been inserted between the *env* gene and 3' UTR, and the U3 region of the 5' long terminal repeat has been replaced by the cytomegalovirus promoter (CMV).  $\psi^+$ , packaging signal; U3/R/U5, domains of viral long terminal repeat; *gag/pol/amphi env*, coding sequences of amphotropic virus. B, *in vitro* replication kinetics in human colon cancer cell lines. To examine replication kinetics, WiDr and LoVo cell lines were infected with replication-competent ACE-GFP vector at an MOI of 0.01 and analyzed for GFP expression by flow cytometry every third day after virus infection.

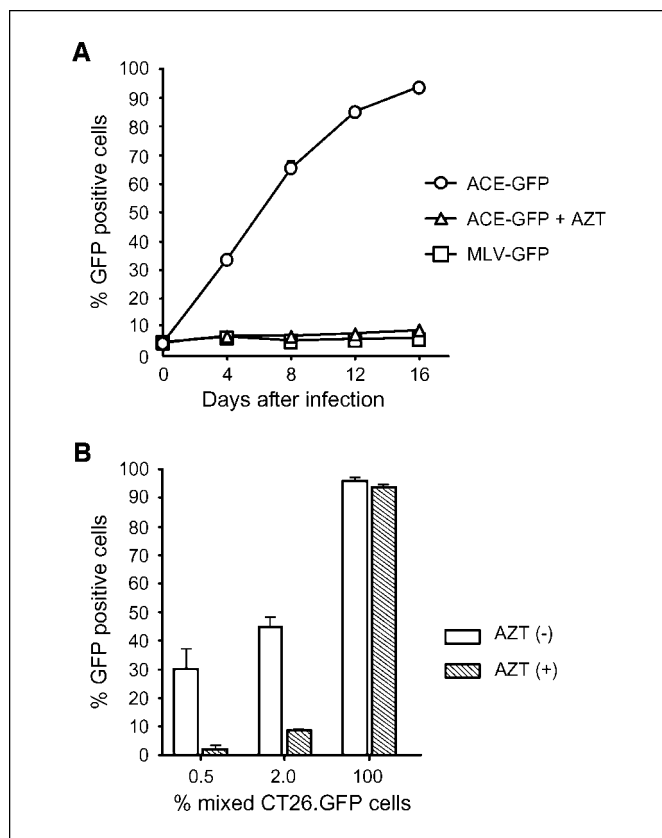


**Figure 2.** *A*, *in vitro* replication kinetics in murine colorectal cancer cell line CT26. To examine replication kinetics, CT26 cells were infected with RCR vector (ACE-GFP) or replication-defective vector (MLV-GFP) at an MOI of 0.05 and analyzed for GFP expression by flow cytometry every 4 d after addition of vector for a period of 16 d. As a control, AZT was added to the medium of cells infected with ACE-GFP to inhibit viral replication (ACE-GFP + AZT). *B*, replicative spread of ACE-GFP in s.c. CT26 tumor model. Parental (CT26) and fully transduced (CT26.GFP) cells were mixed at various ratios (0.5%, 2%, and 100%, as indicated), and these CT26 cell mixtures ( $5 \times 10^4$  cells each) were s.c. inoculated in BALB/c mice. Two weeks later, s.c. tumors were excised, digested, and analyzed by flow cytometry to quantitate GFP expression. As a control group, half of the mice were exposed to AZT (0.4 mg/mL) in the drinking water starting at 1 d before tumor cell inoculation.

protease inhibitor cocktail (Sigma). Subsequently, the lysed cells were centrifuged, and the supernatant was stored at  $-80^{\circ}\text{C}$ . One hundred micrograms of cell lysate from each sample was subjected to SDS-PAGE using 4% to 20% linear gradient gels (Bio-Rad), and the protein was transferred to polyvinylidene difluoride membranes (Amersham). For Western blotting, sheep polyclonal antiyeast CD antibody (1:500; Bio-Trend) was used as the primary antibody and peroxidase-conjugated rabbit anti-sheep antibody (1:20,000; Jackson Immuno Research) was used as the secondary antibody. Chemiluminescent detection of bound antibody was done using the ECL PLUS system (Amersham). Antiactin antibody (1:250; Sigma) was also used as an internal control.

**Cytotoxicity assay *in vitro*.** Cell viability was determined using a tetrazolium dye conversion [3-(4,5-dimethylthiazol-2-yl)-5-(3-carboxymethoxyphenyl)-2-(4-sulfophenyl)-2H-tetrazolium salt (MTS)] assay (Promega). To assess drug cytotoxicity, triplicate wells containing parental CT26, CT26.GFP, or CT26.CD cells ( $2 \times 10^3$  cells per well) were cultured in 96-well plates with various concentrations of 5FC. On day 5, dye conversion was measured using an ELISA plate reader at 490 nm after 2 h incubation at  $37^{\circ}\text{C}$ . Cytotoxicity was determined by calculation of the absorbance of viable cells as measured against wells containing no 5FC. In other experiments, CT26 and CT26.CD cells were mixed in various percentages and cocultured in 96-well plates with 1 mmol/L of 5FC, and cell viability was determined by MTS assay as described above 9 days later.

**Suicide gene therapy in s.c. tumor model.** Uninfected parental CT26 cells (99.5%) were mixed with CT26.CD (0.5%) cells, and these cell mixtures ( $5 \times 10^4$  cells in 100  $\mu\text{L}$  PBS) were s.c. injected into each mouse. To inhibit viral replication, AZT was added to the drinking water (0.4 mg/mL) throughout the experiment, starting from 1 day before tumor cell inoculation. I.p. administration of 5FC (500 mg/kg, twice a day) or PBS was started 12 days after tumor cell inoculation. Tumor volumes were calculated by this formula: volume = length  $\times$  width<sup>2</sup>/2.

**Optical imaging analysis.** Bioluminescence in cultured cells or live mice was examined by optical imaging using a cooled CCD system (Xenogen IVIS). Gray-scale background photographic images of the tissues were overlaid with color images of bioluminescent signals using Living Image and IGOR-PRO image analysis software (Wave Metrics). For *in vitro* imaging, firefly luciferase expression in CT26 cells after lentiviral vector transduction ( $1 \mu\text{g}$  p24/1  $\times 10^5$  cells) was confirmed with the Xenogen system 2 min after addition of D-luciferin (150  $\mu\text{g}$ /well). For *in vivo* imaging, mice were anesthetized with ketamine (100 mg/kg) and xylazine (10 mg/kg), and 2 min after i.p. administration with D-luciferin (126 mg/kg), bioluminescent signals were analyzed with the Xenogen system with a 30-s acquisition time.

**Orthotopic liver metastasis models.** A syngeneic mouse model of colorectal cancer metastasis to the liver was also established as previously described (33) by infusion of tumor cells into the portal system via intrasplenic injection. Briefly, after making a left subcostal incision under isoflurane anesthesia, CT26.Fluc cells ( $5 \times 10^4$  cells) in 200  $\mu\text{L}$  PBS were inoculated by intrasplenic injection. For optical living imaging in this model, splenectomy was done immediately after tumor cell inoculation, and the firefly luciferase signal expression was analyzed at various time points with the Xenogen system as above. Immediately after imaging analysis, the liver and disseminated peritoneal tumors were excised, weighed, and processed for histology. Tumor weights were determined by subtracting the average liver weight of normal mice ( $n = 3$ ) from the total tumor-bearing liver weight with addition of the total weight of extrahepatic tumors.

For therapeutic experiments, after anesthesia and a second laparotomy, ACE-CD vector ( $2 \times 10^4$  TU/200  $\mu\text{L}$ ) was also given via intrasplenic injection 3 days after tumor cell inoculation, after which splenectomy was done. I.p. administration of 5FC (500 mg/kg, twice a day) or PBS was started 14 days after tumor cell inoculation. To evaluate tumor growth inhibition, the mice were analyzed every 7 days by optical imaging as described above.

**Quantitative real-time PCR analysis of vector biodistribution.** Genomic DNA was isolated from harvested tissues (tumor, normal liver, and bone marrow) using the DNeasy tissue kit (Qiagen). To detect integrated RCR sequences, quantitative real-time PCR was done in a 25- $\mu\text{L}$  reaction mixture containing genomic DNA, 12.5  $\mu\text{L}$  of  $2\times$  TaqMan Universal PCR Master Mix (PE Applied Biosystems), 300 nmol/L of each primer, and 100 nmol/L of fluorogenic probe. Amplifications were carried out in duplicate using an ABI Prism 7700 sequence detector. After initial denaturation (10 min at  $95^{\circ}\text{C}$ ), amplification was done with 40 cycles of 15 s at  $95^{\circ}\text{C}$  and 60 s at  $60^{\circ}\text{C}$ . A reference curve for retrovirus copy number was prepared by amplifying serial dilutions of CT26.CD genomic DNA in a background of genomic DNA from untransduced bone marrow and plotting Ct values against the input CT26.CD DNA. The threshold for vector detection was determined by a control sample with no CT26.CD DNA. The primers and probe were designed to target the 4070A amphotropic *env* gene (4070A-F, 5'-GCGGACCCGACTTTTGA-3'; 4070A-R, 5'-ACCCCGACTTTACGGTATGC-3'; probe, FAM-CAGGGCACACGTAATAA-NFQ). Mouse  $\beta$ -actin was also quantified as an internal control gene ( $\beta$ -actin-F, 5'-GGTCGTACCACAGGATTGT-3';  $\beta$ -actin-R, 5'-CTCGTAGATGGG-CACAGTGT-3'; probe, FAM-CCCGTCTCCGGAGTCC-NFQ).

**Statistical analysis.** Statistical analyses were done with Student's *t* test or one-way ANOVA to determine significance. Coefficient of determination ( $r^2$ ) values  $>0.9$  were defined as a strong correlation. *P* values of  $<0.05$  were considered statistically significant in all analyses, which were done with Prism 4 statistical software (GraphPad Software).

## Results

**RCR vectors replicate efficiently in human and murine colorectal cancer cells *in vitro* and *in vivo*.** To examine replication kinetics in human and murine colon cancer cells, we first used the MLV-based RCR vector ACE-GFP (20, 32), which contains an IRES-GFP cassette inserted precisely at the *env*-3' untranslated region (UTR) boundary (Fig. 1A). GFP expression was monitored by flow cytometry at serial time points after inoculation of cultures of WiDr and LoVo cells with ACE-GFP at an MOI of 0.01. In both cell lines, the percentage of GFP-expressing cells quickly increased in a logarithmic manner and reached >80% within 12 to 27 days after virus inoculation (Fig. 1B), and then remained stable thereafter. Replication kinetics were also examined in murine colon cancer CT26 cells at serial time points after ACE-GFP infection (initial dose, MOI = 0.05) in the presence or absence of AZT (Fig. 2A). The initial percentage of GFP-expressing CT26 cells at 24 h after infection with either ACE-GFP or the conventional replication-defective retroviral vector MLV-GFP was confirmed to be ~5% by flow cytometry. Subsequently, the percentage of GFP-positive CT26 cells in the ACE-GFP-infected group increased rapidly, reaching >95% within 16 days. This significant increase was due to viral replication as it could be completely inhibited by addition of AZT, a potent inhibitor of retrovirus replication (39). As expected, in the group infected with the nonreplicating vector MLV-GFP, no increase in the percentage of GFP-positive cells was observed over time.

To evaluate the replicative spread of RCR vectors *in vivo*, cell suspensions consisting of mixtures of parental (CT26) and transduced (CT26.GFP) cells in various ratios (0.5%, 2%, and 100%) were used to establish s.c. tumor models. Fourteen days after s.c. inoculation of each mixed cell suspension in syngeneic BALB/c mice, tumors were excised and analyzed by flow cytometry (Fig. 2B). Consistent with the results of the *in vitro* studies even

in tumors starting with only 0.5% CT26.GFP cells, the percentage of GFP-positive tumor cells increased to >30% within 14 days. Replicative spread of the ACE-GFP vector was effectively prevented in the 0.5% and 2% CT26.GFP tumors by AZT administration *in vivo* but did not affect GFP expression from pretransduced cells as the 100% CT26.GFP group maintained stable expression of the transgene.

**RCR vectors mediate efficient delivery and functional expression of the yeast CD suicide gene in murine colorectal cancer cells *in vitro*.** For suicide gene therapy, we developed another MLV-based RCR vector, ACE-CD, which expresses the yeast CD suicide gene (ref. 32; Fig. 3A), and used it to stably transduce CT26 cells *in vitro*. Complete transduction of the entire cell population was ensured by monitoring a parallel culture of CT26 cells infected with ACE-GFP under the same conditions. The transduction efficiency of the ACE-CD vector was also confirmed directly to be >97% by quantitative real-time PCR analysis of infected CT26 cells, using primers targeting the amphotropic envelope gene. Strong expression of the yeast CD protein was confirmed in this stably transduced cell population (CT26.CD) by Western blot (Fig. 3B). No significant differences in growth rate were observed between parental CT26 and CT26.CD (data not shown).

As the CD enzyme converts the nontoxic prodrug 5FC into the chemotoxin FU inside infected tumor cells, *in vitro* cytotoxicity was then examined by MTS assay after exposure of transduced cells to the 5FC prodrug at various concentrations (Fig. 3C). Control cells transduced with ACE-GFP (CT26.GFP) showed little loss of viability at lower concentrations of 5FC up to 1 mmol/L and <20% growth inhibition even after 10 mmol/L 5FC treatment. In contrast, the viability of CT26.CD cells was reduced by over 80% even after exposure to only 0.1 mmol/L of 5FC, and complete cell killing was observed after 5 days of exposure to 10 mmol/L of the prodrug.

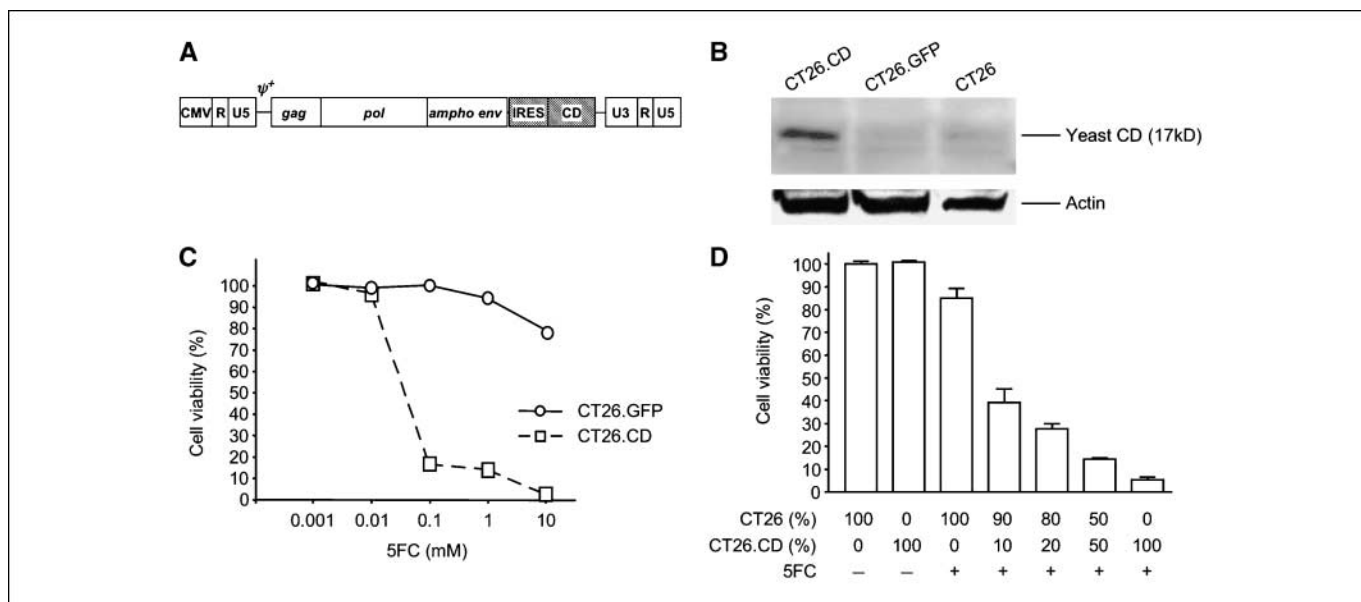
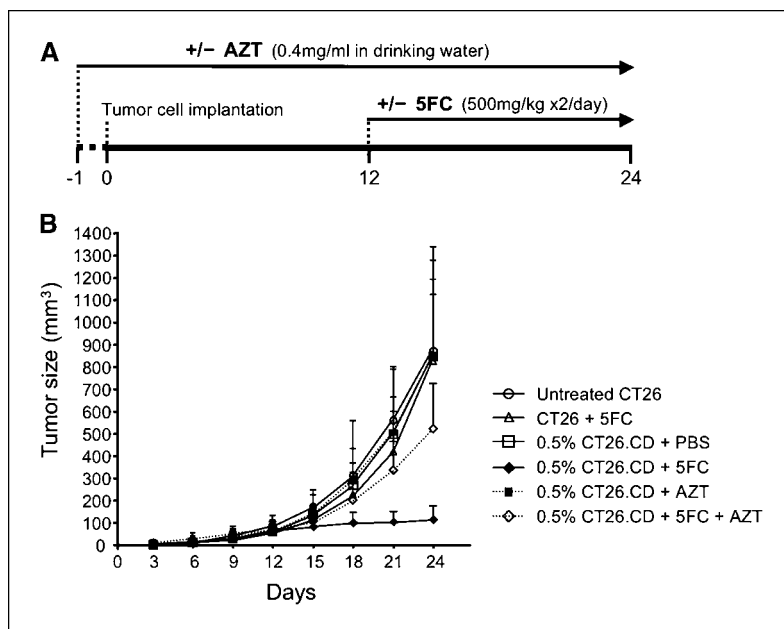


**Figure 3.** A, design of RCR vector ACE-CD. The IRES-GFP cassette of pACE-GFP was replaced with an IRES-CD cassette. Other abbreviations are as in Fig. 1. B, yeast CD expression in CT26 cells infected with ACE-CD vector. Western blots of extracts from cells that were fully transduced with ACE-CD (CT26.CD) or ACE-GFP (CT26.GFP) or untransduced parental CT26 cells (CT26) were probed with antiyeast CD antibody (yeast CD), or antiactin antibody as an internal control (actin). C, *in vitro* MTS assay to assess 5FC drug cytotoxicity in CT26.GFP versus CT26.CD cells. Cell viability was measured by MTS dye conversion after exposure to 5FC at the indicated concentrations and normalized to nontransduced parental CT26 cells. D, untransduced parental CT26 and CT26.CD cells were mixed at various percentages, as indicated, and treated with 1 mmol/L of 5FC. Cell viability was determined 9 d later by MTS assay as above.

**Figure 4.** RCR-mediated CD/5FC suicide gene therapy inhibits growth of syngeneic CT26 s.c. tumor in immunocompetent BALB/c mice. **A**, schematic representation of the schedule of drug administration for the s.c. tumor model. For AZT control groups, mice were exposed to AZT (0.4 mg/mL) in the drinking water starting at 1 d before tumor cell inoculation. For 5FC treatment groups, i.p. 5FC administration was started 12 d after tumor cell inoculation. **B**, uninfected parental CT26 cells (99.5%) were mixed with transduced CT26.CD cells (0.5%), and these CT26 cell mixtures or parental CT26 control cells were s.c. injected into each mouse. Treatment with 5FC prodrug and/or AZT was done as indicated according to the schedule shown above. On day 24, significant differences were observed between the 0.5% CT26.CD + 5FC group and the other control groups ( $P = 0.0001$ ;  $n = 8$ ).



The above experiments were done with a pure population of fully transduced CT26.CD cells. Next, parental (CT26) and pretransduced (CT26.CD) cells were mixed at various ratios (10%, 20%, and 50% CT26.CD) and cocultured for 24 h (Fig. 3D), followed by addition of 5FC prodrug at the highest dose showing the least nonspecific toxicity determined above (1 mmol/L), and cell viability was assessed by MTS assay on day 9. As expected, even without 5FC treatment 100% CT26.CD cell populations showed no growth retardation compared with parental CT26 cells. As found previously, nontransduced parental CT26 cells showed <20% loss of viability after 5FC treatment. In contrast, >50% cell death was observed in all mixed cell populations even with an initial ratio of only 10% CT26.CD cells, with progressive increases in cytotoxicity associated with increasing initial percentages of CT26.CD cells.

**RCR vector-mediated CD/5FC suicide gene therapy shows potent antitumor effects in s.c. CT26 tumors *in vivo*.** We first evaluated the therapeutic efficacy of RCR-mediated suicide gene therapy using s.c. CT26 tumors established in immunocompetent syngeneic mice (Fig. 4A). For this model, parental CT26 cells and pretransduced CT26.CD cells were mixed at the lowest percentage of transduction used in the previous ACE-GFP s.c. tumor experiments (i.e., 0.5% CT26.CD cells), and this cell mixture was s.c. injected in BALB/c mice as above. Twelve days after tumor cell inoculation, i.p. 5FC administration (500 mg/kg, twice daily) was initiated. Mice bearing ACE-CD transduced tumors without 5FC treatment (0.5% CT26.CD + PBS group; Fig. 4B), as well as mice receiving 5FC treatment without virus transduction (parental CT26 + 5FC group; Fig. 4B), showed no obvious inhibition of tumor growth compared with control nontreated mice with nontransduced tumors (parental CT26 + PBS group; Fig. 4B). However, the growth of ACE-CD transduced tumors was significantly inhibited by 5FC treatment after day 12 (0.5% CT26.CD + 5FC group). This antitumor effect required active virus replication, as the inhibitory effect was significantly diminished when AZT was given to the animals (0.5% CT26.CD + 5FC + AZT group; Fig. 4B). AZT itself had no detectable effect on tumor growth (0.5% CT26.CD + AZT; Fig. 4B).

#### Validation of live imaging using CT26 cells expressing firefly luciferase in an orthotopic multifocal liver metastasis model.

To allow assessment of the therapeutic effect of RCR vector-mediated suicide gene therapy in individual animals using an orthotopic CT26 multifocal liver metastasis model which we have used previously (33), we first prepared CT26 cells pretransduced with a conventional replication-defective lentivirus vector expressing firefly luciferase (CT26.Fluc). Stable expression of luciferase in these cells was confirmed by optical imaging *in vitro* (Fig. 5A), which showed a quantitative correlation between CT26.Fluc cell number and luminescent signal intensity.

We then examined the correlation between optical imaging signals in living animals and tumor burden in the orthotopic multifocal liver metastasis model (Fig. 5B and C). The firefly luciferase signal intensity was analyzed at various time points. And at each time point, both hepatic and extrahepatic metastatic tumor foci were excised and weighed immediately after imaging. There was a strong quantitative correlation ( $r^2 = 0.93$ ,  $P < 0.0001$ ) between the bioluminescent signal intensity and total tumor weight, which validated optical imaging as an accurate method for longitudinal monitoring of changes in tumor burden in the same animal after therapeutic interventions in this model.

**CD/5FC suicide gene therapy by locoregional delivery of RCR vectors achieves significant inhibition of orthotopic multifocal liver metastases.** *In vivo* efficacy of RCR-mediated suicide gene therapy was then assessed in the orthotopic metastasis model using CT26.Fluc cells inoculated via splenic injection as above to form multiple tumor foci in the livers of syngeneic BALB/c mice. On day 3 after tumor establishment, a total dose of  $2 \times 10^4$  TU ACE-CD virus supernatant in 200  $\mu$ L total volume was given by locoregional infusion via the same route, and each mouse was analyzed by optical imaging on days 7, 14, 21, and 28 (Fig. 6). I.p. 5FC prodrug treatment was commenced on day 14 (ACE-CD + 5FC group; Fig. 6). Control mice received PBS vehicle only instead of 5FC or were untreated (ACE-CD + PBS group and untreated group; Fig. 6). All animals in both control groups showed tumor progression as evidenced by increasing bioluminescence

signal intensities, but the group treated with ACE-CD followed by 5FC showed animals exhibited stable disease or decreased tumor burden in five of seven animals, and minimal progression in the remaining animals; overall, average tumor growth was significantly inhibited compared with controls. By day 28 after virus infusion, the ACE-CD + 5FC group showed significant signal inhibition compared with the control groups ( $P < 0.05$ ). Histologically, areas of tumor showed extensive necrosis, but there were no pathologic changes noted in the normal liver parenchyma of these animals (data not shown).

**No detectable RCR vector spread to intact liver tissue or bone marrow.** For rigorous detection of any possible RCR vector

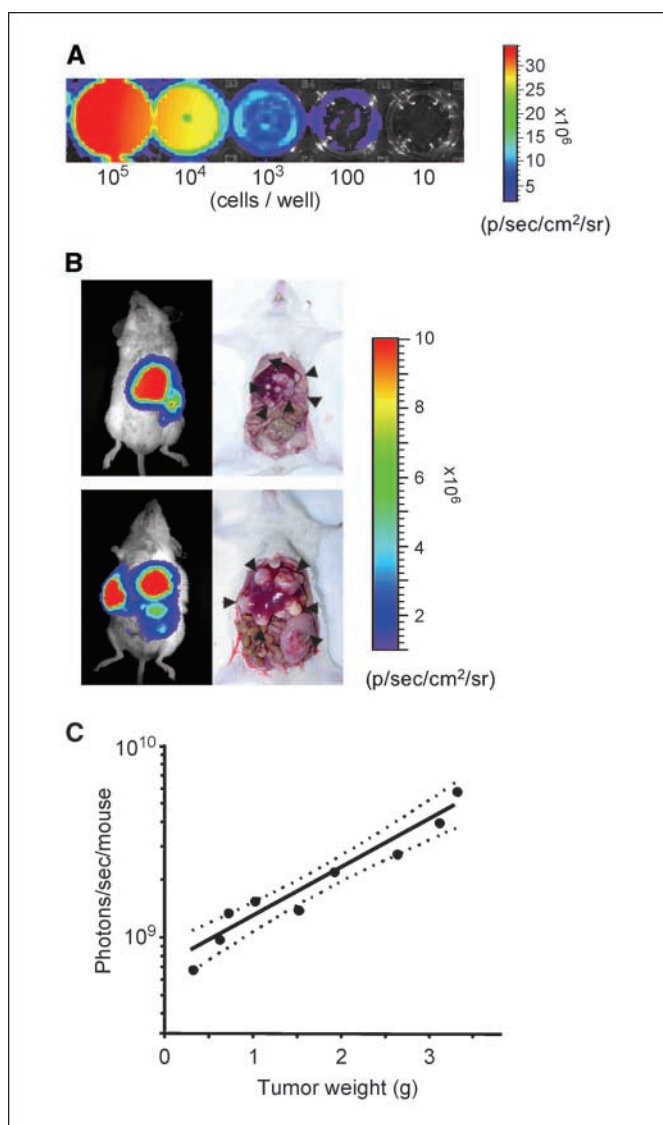


**Figure 5.** Bioluminescence imaging of CT26 tumors *in vivo*. **A**, CT26 cells engineered to express firefly luciferase by lentiviral transduction (CT26.Fluc) were examined by optical imaging. **B**, representative examples comparing bioluminescence imaging results and actual tumor masses (indicated by arrows) in the same animal. Note that imaging results may vary from location of tumors due to shifting after dissection. **C**, relationship between bioluminescence signals and actual weights of tumors in CT26.Fluc syngeneic hepatic metastasis model. After optical imaging at various time points, the hepatic and extrahepatic tumors were immediately excised and weighed, and the signal intensities (photons per second per mouse) were plotted against tumor weights (g). *Solid line*, linear regression curve; *dashed lines*, 95% confidence interval ( $r^2 = 0.93$ ;  $P < 0.0001$ ).

spread to normal organs, quantitative real-time PCR analysis of genomic DNA extracted from liver tumor, normal liver tissue, or bone marrow was done using primers and probe sequences specific for the 4070A amphotropic envelope (Table 1). This method was determined to be sensitive enough to detect 20 copies of the RCR provirus per  $5 \times 10^4$  cellular genomes. Genomic DNA from ACE-CD-transduced metastatic CT26.Fluc tumor tissues showed robust amplification of proviral RCR sequences, which were quantitated to range between 16% and 32% transduction levels by copy number. This level of transduction is consistent with the transduction efficiency observed previously using ACE-GFP in orthotopic CT26 hepatic metastases (33). However, no detectable RCR signals were observed in genomic DNA from uninvolved normal liver or bone marrow tissues after locoregional administration of ACE-CD, either with or without prodrug treatment, indicating that RCR vector replication was confined to the tumor tissues.

## Discussion

In the present study, we showed that the RCR vector ACE-CD could replicate efficiently in colorectal cancer cells *in vitro* and *in vivo* while preserving the enzymatic function of CD, and mediated significant growth inhibition of both s.c. and multifocal orthotopic CT26 tumors was observed after virus injection at doses as low as  $2 \times 10^4$  TU followed by 5FC prodrug administration. In the s.c. tumor model, growth inhibition was strongly blocked by AZT administration, indicating that this significant therapeutic effect required efficient RCR vector replication. This result is consistent with our previous report demonstrating efficient replication of a marker gene RCR vector, ACE-GFP, in both human and murine colorectal cancer cells *in vitro*, and that locoregional infusion of RCR vectors via the portal circulation can initiate highly efficient intratumoral virus replication and gene delivery in this multifocal orthotopic metastasis model (33).

In a previous study, systemic FU administration in the same CT26 multiple liver metastasis model under conditions similar to those used in the present study was reported to show no therapeutic efficacy compared with control mice despite continuous infusion of FU at the maximum tolerated dose via osmotic pump (100 mg/kg/2 weeks; ref. 36). As systemic infusion of the prodrug 5FC, a Food and Drug Administration-approved antifungal agent, is relatively nontoxic and results in direct intracellular conversion to FU only in the RCR vector-infected tumor cells, this strategy has the potential to be more efficacious and less toxic than conventional chemotherapy with systemic FU, and in the clinical setting, could enhance the therapeutic index of combination regimens that currently include FU. Additionally, 5FC administration may also selectively kill any normal actively dividing cells that might have been inadvertently transduced by the RCR vector.

By use of live bioluminescence optical imaging, tumors in the same individual can be sequentially visualized and tumor volume quantified, as has been reported in various tumor models (40–43). On the other hand, in orthotopic multiple liver metastasis models, evaluations have usually been done by counting the number of tumor foci by macroscopic or histopathologic examination and/or measuring the total tumor or liver weight (10, 27, 44, 45). Whereas a previous report has validated the use of bioluminescence imaging in a murine orthotopic colorectal cancer metastasis model (43), to our knowledge, there has been only one other report of using this technique to monitor the therapeutic efficacy of suicide gene

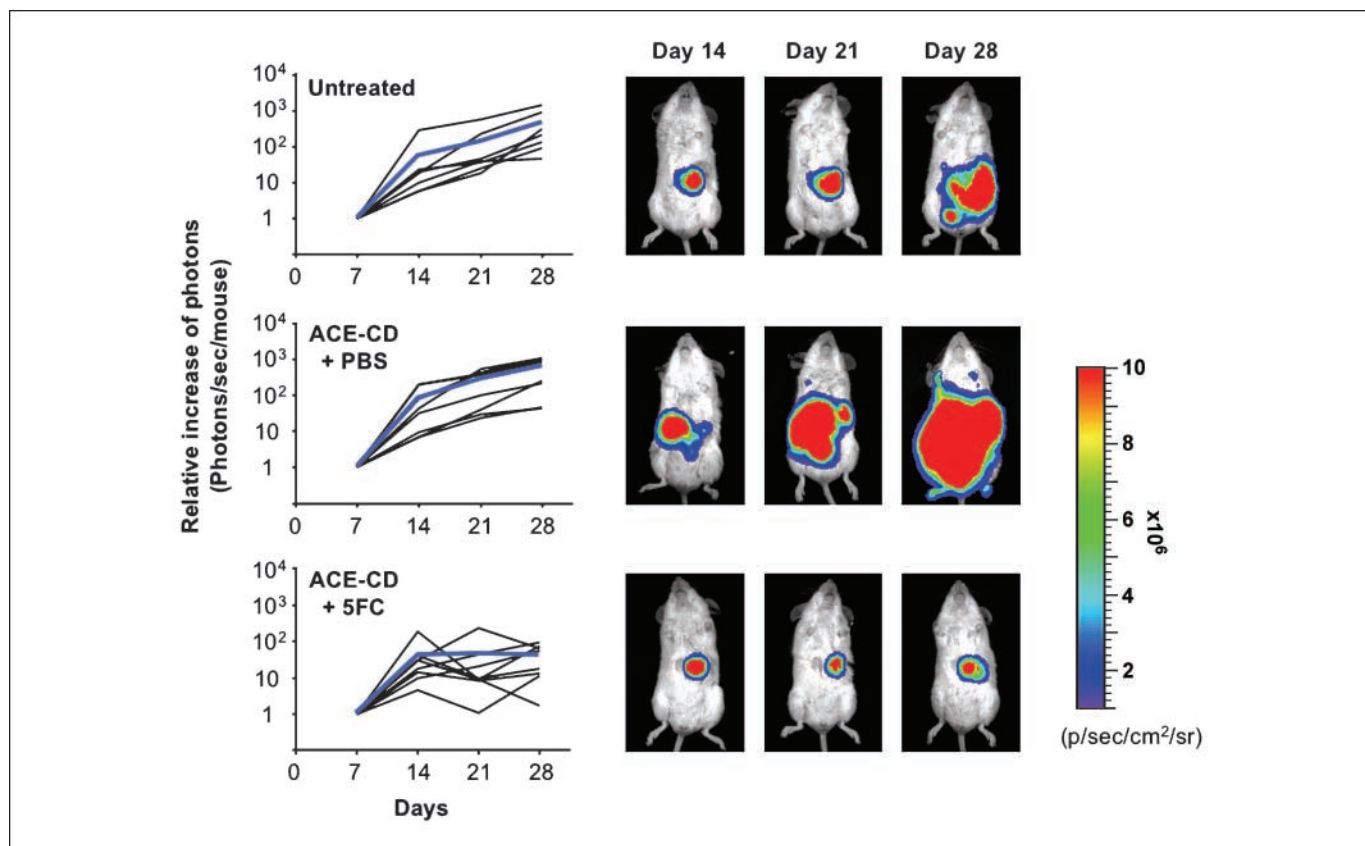


**Figure 6.** Effect of 5FC after locoregional delivery of RCR in orthotopic multifocal liver metastasis model. On day 3 after tumor establishment,  $2 \times 10^4$  TU ACE-CD virus supernatant was infused via the portal circulation, and the mice were analyzed by optical bioluminescence imaging on days 7, 14, 21, and 28. I.p. 5FC administration (500 mg/kg, twice a day) was started on day 14 (ACE-CD + 5FC group). Control groups received no vector (untreated) or received vector followed by PBS instead of prodrug (ACE-CD + PBS). *Black curves*, signal intensities recorded from individual animals; *blue curves*, average signal intensity for each group. The average signal intensity of ACE-CD + 5FC treated mice was significantly weaker than that in control mice ( $P < 0.05$ ) at day 28 after tumor cell inoculation (*left*). Each row of images to the right of the graphs shows representative imaging results from each group of the same animal at different time points (*right*).

therapy in such a model (12), and in this previous report, the hepatic tumors had been 10% or 100% pretransduced with a conventional retrovirus vector and were implanted as solitary lesions by direct intrahepatic tumor inoculation. Therefore, to our knowledge, this represents the first report to use live imaging to

monitor suicide gene therapy using a multifocal orthotopic colorectal cancer metastasis model, particularly with the use of a replicating vector. In this orthotopic model, a significant linear correlation could be observed between the strength of the photon signal and the actual tumor weight and allowed the use of this

**Table 1.** Biodistribution of RCR vector after locoregional virus infusion in immunocompetent CT26 hepatic metastasis model

Copy number of RCR vector *in vivo*

Vector	Prodrug	Number of vector copies per $5 \times 10^4$ cells		
		Tumor	Liver	Bone marrow
No vector	Untreated	—	—	—
No vector	Untreated	—	—	—
ACE-CD	PBS	16,623	—	—
ACE-CD	PBS	11,223	—	—
ACE-CD	5FC	8,066	—	—
ACE-CD	5FC	11,174	—	—

NOTE: Genomic DNA, extracted from liver tumor, normal liver, or bone marrow of ACE-GFP infected mice, was analyzed by quantitative real-time PCR as described in Materials and Methods. As an internal control, each sample was also amplified with mouse  $\beta$ -actin specific primers.

Abbreviation: —, not detectable (detection limit was 20 copies per  $5 \times 10^4$  cells).

method to follow-up variations of tumor volume in each live mouse.

Suicide gene therapy using replication-defective virus vectors expressing CD in hepatic tumor models have been reported previously to achieve significant transduction levels and therapeutic effect, but many of these studies were done using solitary tumor models established by direct intrahepatic inoculation (11–13, 30). Whereas a number of studies have also reported the therapeutic efficacy of replicating viruses in multifocal metastasis models both through intrinsic oncolytic activity and with augmentation using suicide genes, such as CD, the possibility of cytolytic or cytotoxic damage to adjacent normal liver cells or other normal tissues still remains (29, 30, 46) even with the use of transcriptional targeting (13). On the other hand, MLV-based RCR vectors, even without specific targeting, possess tumor selectivity due to an inherent and stringent specificity for mitotically active cells and, hence, can only infect cells that are actively dividing (23). In the present study, no obvious ACE-CD vector integration was detected in extratumoral normal liver tissue or bone marrow by sensitive real-time PCR methods. This result is also consistent with our previous study showing that the marker gene RCR vector ACE-GFP delivered to orthotopic liver tumors via locoregional delivery in immunocompetent syngeneic hosts showed no detectable spread to normal tissues, including peritumoral normal liver tissue, bone marrow, lung, kidney, small intestine, and colon (33). Whereas normal liver tissue is quiescent, bone marrow does contain actively dividing cells; but RCR spread to bone marrow presumably requires systemic hematogenous spread of the virus at higher levels, and direct i.v. infusion of wild-type MLV is known to result in infection of bone marrow and spleen in immunodeficient and immunologically immature neonatal mice, but not in adult immunocompetent mice (47).

In the present study, although significant growth inhibition of tumors was achieved, complete regression of tumors was not obtained. We have previously reported that the transduction level of among different tumor nodules in this multifocal model was

variable after locoregional infusion; and because of the highly aggressive nature of CT26 tumor growth, the virus could spread for only a limited period of time before the tumor burden became lethal (33). Our current results suggest that some tumor nodules with sufficiently low levels of RCR transduction might survive and grow despite any bystander effect and, thus, offset the antitumor effect achieved in the highly transduced tumor nodules. However, the doses used in the present study were quite low, on the order of  $10^4$  TU, and higher initial transduction levels would presumably result in faster replication kinetics and improved overall tumor transduction levels in every nodule. Furthermore, in a clinical setting, even if complete responses are not achieved, the use of RCR vector-mediated suicide gene therapy as a relatively nontoxic neoadjuvant could reduce tumor burden sufficiently to convert an unresectable case to one that may be amenable to subsequent surgical removal. In addition, it should be noted that the unique property of stable integration by RCR vectors results in continual intratumoral production of virus progeny; hence, longer patient survival achieved by combination with other treatments, such as conventional chemotherapy or newer biological therapies, should allow higher levels of suicide gene expression even in initially poorly transduced tumor nodules; even a short prolongation of patient survival during the logarithmic phase spread of the virus may significantly enhance intratumoral transduction levels. Subsequently, recurrent malignant cells that escaped initial prodrug treatment or other treatments might then be killed by repeated administration of prodrug at later time points.

## Acknowledgments

Received 12/20/2006; revised 3/8/2007; accepted 4/6/2007.

**Grant support:** NIH grants P01CA59318 (Project 2), R01CA105171 (N. Kasahara), Susan G. Komen Breast Cancer Foundation (K. Hiraoka), and National Cancer Institute grant R25 CA098010 (C. Logg).

The costs of publication of this article were defrayed in part by the payment of page charges. This article must therefore be hereby marked *advertisement* in accordance with 18 U.S.C. Section 1734 solely to indicate this fact.

## References

- Jemal A, Siegel R, Ward E, et al. Cancer statistics, 2006. *CA Cancer J Clin* 2006;56:106–30.
- Bentrem DJ, Dematteo RP, Blumgart LH. Surgical therapy for metastatic disease to the liver. *Annu Rev Med* 2005;56:139–56.
- Mayer-Kuckuk P, Banerjee D, Kemeny N, Fong Y, Bertino JR. Molecular therapies for colorectal cancer metastatic to the liver. *Mol Ther* 2002;5:492–500.
- Wagner JS, Adson MA, Van Heerden JA, Adson MH, Ilstrup DM. The natural history of hepatic metastases from colorectal cancer. A comparison with resective treatment. *Ann Surg* 1984;199:502–8.
- Douillard JY, Cunningham D, Roth AD, et al. Irinotecan combined with fluorouracil compared with fluorouracil alone as first-line treatment for metastatic colorectal cancer: a multicentre randomised trial. *Lancet* 2000;355:1041–7.
- Kohne CH, van Cutsem E, Wils J, et al. Phase III study of weekly high-dose infusional fluorouracil plus folinic acid with or without irinotecan in patients with metastatic colorectal cancer: European Organisation for Research and Treatment of Cancer Gastrointestinal Group Study 40986. *J Clin Oncol* 2005;23:4856–65.
- Saltz LB, Cox JV, Blanke C, et al. Irinotecan plus fluorouracil and leucovorin for metastatic colorectal cancer. Irinotecan Study Group. *N Engl J Med* 2000;343:905–14.
- de Gramont A, Figer A, Seymour M, et al. Leucovorin and fluorouracil with or without oxaliplatin as first-line treatment in advanced colorectal cancer. *J Clin Oncol* 2000;18:2938–47.
- Grothey A, Sargent D, Goldberg RM, Schmoll HJ. Survival of patients with advanced colorectal cancer improves with the availability of fluorouracil-leucovorin, irinotecan, and oxaliplatin in the course of treatment. *J Clin Oncol* 2004;22:1209–14.
- Block A, Freund CT, Chen SH, et al. Gene therapy of metastatic colon carcinoma: regression of multiple hepatic metastases by adenoviral expression of bacterial cytosine deaminase. *Cancer Gene Ther* 2000;7:438–45.
- Chen SH, Chen XH, Wang Y, et al. Combination gene therapy for liver metastasis of colon carcinoma *in vivo*. *Proc Natl Acad Sci U S A* 1995;92:2577–81.
- Nyati MK, Symon Z, Kievit E, et al. The potential of 5-fluorocytosine/cytosine deaminase enzyme prodrug gene therapy in an intrahepatic colon cancer model. *Gene Ther* 2002;9:844–9.
- Zhang M, Li S, Nyati MK, et al. Regional delivery and selective expression of a high-activity yeast cytosine deaminase in an intrahepatic colon cancer model. *Cancer Res* 2003;63:658–63.
- Sung MW, Yeh HC, Thung SN, et al. Intratumoral adenovirus-mediated suicide gene transfer for hepatic metastases from colorectal adenocarcinoma: results of a phase I clinical trial. *Mol Ther* 2001;4:182–91.
- Dalba C, Klatzmann D, Logg CR, Kasahara N. Beyond oncolytic virotherapy: replication-competent retrovirus vectors for selective and stable transduction of tumors. *Curr Gene Ther* 2005;5:655–67.
- Parato KA, Senger D, Forsyth PA, Bell JC. Recent progress in the battle between oncolytic viruses and tumours. *Nat Rev Cancer* 2005;5:965–76.
- Sze DY, Freeman SM, Slonim SM, et al. Dr. Gary J. Becker Young Investigator Award: intraarterial adenovirus for metastatic gastrointestinal cancer: activity, radiographic response, and survival. *J Vasc Interv Radiol* 2003;14:279–90.
- Reid T, Galanis E, Abbruzzese J, et al. Hepatic arterial infusion of a replication-selective oncolytic adenovirus (dl1520): phase II viral, immunologic, and clinical endpoints. *Cancer Res* 2002;62:6070–9.
- Logg CR, Kasahara N. Retrovirus-mediated gene transfer to tumors: utilizing the replicative power of viruses to achieve highly efficient tumor transduction *in vivo*. *Methods Mol Biol* 2004;246:499–525.
- Logg CR, Logg A, Matusik RJ, Bochner BH, Kasahara N. Tissue-specific transcriptional targeting of a replication-competent retroviral vector. *J Virol* 2002;76:12783–91.
- Logg CR, Logg A, Tai CK, Cannon PM, Kasahara N. Genomic stability of murine leukemia viruses containing insertions at the Env-3' untranslated region boundary. *J Virol* 2001;75:6989–98.
- Logg CR, Tai CK, Logg A, Anderson WF, Kasahara N.



- A uniquely stable replication-competent retrovirus vector achieves efficient gene delivery *in vitro* and in solid tumors. *Hum Gene Ther* 2001;12:921–32.
23. Miller DG, Adam MA, Miller AD. Gene transfer by retrovirus vectors occurs only in cells that are actively replicating at the time of infection. *Mol Cell Biol* 1990;10:4239–42.
  24. Habib NA, Sarraf CE, Mitry RR, et al. E1B-deleted adenovirus (dl1520) gene therapy for patients with primary and secondary liver tumors. *Hum Gene Ther* 2001;12:219–26.
  25. Sagawa T, Takahashi M, Sato T, et al. Prolonged survival of mice with multiple liver metastases of human colon cancer by intravenous administration of replicable E1-55K-deleted adenovirus with E1A expressed by CEA promoter. *Mol Ther* 2004;10:1043–50.
  26. Kooby DA, Carew JF, Halterman MW, et al. Oncolytic viral therapy for human colorectal cancer and liver metastases using a multmutated herpes simplex virus type-1 (G207). *FASEB J* 1999;13:1325–34.
  27. Reinblatt M, Pin RH, Federoff HJ, Fong Y. Utilizing tumor hypoxia to enhance oncolytic viral therapy in colorectal metastases. *Ann Surg* 2004;239:892–9;discussion 899–902.
  28. Reinblatt M, Pin RH, Fong Y. Carcinoembryonic antigen directed herpes viral oncolysis improves selectivity and activity in colorectal cancer. *Surgery* 2004;136:579–84.
  29. Gnant MF, Puhlmann M, Alexander HR, Jr., Bartlett DL. Systemic administration of a recombinant vaccinia virus expressing the cytosine deaminase gene and subsequent treatment with 5-fluorocytosine leads to tumor-specific gene expression and prolongation of survival in mice. *Cancer Res* 1999;59:3396–403.
  30. Gnant MF, Puhlmann M, Bartlett DL, Alexander HR, Jr. Regional versus systemic delivery of recombinant vaccinia virus as suicide gene therapy for murine liver metastases. *Ann Surg* 1999;230:352–60.
  31. Tai CK, Wang WJ, Chen TC, Kasahara N. Single-shot, multicycle suicide gene therapy by replication-competent retrovirus vectors achieves long-term survival benefit in experimental glioma. *Mol Ther* 2005;12:842–51.
  32. Wang WJ, Tai CK, Kasahara N, Chen TC. Highly efficient and tumor-restricted gene transfer to malignant gliomas by replication-competent retroviral vectors. *Hum Gene Ther* 2003;14:117–27.
  33. Hiraoka K, Kimura T, Logg CR, Kasahara N. Tumor-selective gene expression in a hepatic metastasis model after locoregional delivery of a replication-competent retrovirus vector. *Clin Cancer Res* 2006;12:7108–16.
  34. Humphreys MJ, Ghaneh P, Greenhalf W, et al. Hepatic intra-arterial delivery of a retroviral vector expressing the cytosine deaminase gene, controlled by the CEA promoter and intraperitoneal treatment with 5-fluorocytosine suppresses growth of colorectal liver metastases. *Gene Ther* 2001;8:1241–7.
  35. Nyati MK, Sreekumar A, Li S, et al. High and selective expression of yeast cytosine deaminase under a carcinoembryonic antigen promoter-enhancer. *Cancer Res* 2002;62:2337–42.
  36. Stoeltzing O, Liu W, Reinmuth N, et al. Inhibition of integrin  $\alpha 5\beta 1$  function with a small peptide (ATN-161) plus continuous 5-FU infusion reduces colorectal liver metastases and improves survival in mice. *Int J Cancer* 2003;104:496–503.
  37. Cannon PM, Kim N, Kingsman SM, Kingsman AJ. Murine leukemia virus-based Tat-inducible long terminal repeat replacement vectors: a new system for anti-human immunodeficiency virus gene therapy. *J Virol* 1996;70:8234–40.
  38. Stripecke R, Koya RC, Ta HQ, Kasahara N, Levine AM. The use of lentiviral vectors in gene therapy of leukemia: combinatorial gene delivery of immunomodulators into leukemia cells by state-of-the-art vectors. *Blood Cells Mol Dis* 2003;31:28–37.
  39. Mitsuya H, Broder S. Strategies for antiviral therapy in AIDS. *Nature* 1987;325:773–8.
  40. Thorne SH, Negrin RS, Contag CH. Synergistic antitumor effects of immune cell-viral biotherapy. *Science* 2006;311:1780–4.
  41. Chan JK, Hamilton CA, Cheung MK, et al. Enhanced killing of primary ovarian cancer by retargeting autologous cytokine-induced killer cells with bispecific antibodies: a preclinical study. *Clin Cancer Res* 2006;12:1859–67.
  42. Drake JM, Gabriel CL, Henry MD. Assessing tumor growth and distribution in a model of prostate cancer metastasis using bioluminescence imaging. *Clin Exp Metastasis* 2005;22:674–84.
  43. Smakman N, Martens A, Kranenburg O, Borel Rinkes IH. Validation of bioluminescence imaging of colorectal liver metastases in the mouse. *J Surg Res* 2004;122:225–30.
  44. Tanji H, Yahata H, Hayamizu K, et al. Augmentation of local antitumor immunity in liver by interleukin-2 gene transfer via portal vein. *Cancer Gene Ther* 2002;9:655–64.
  45. Sova P, Ren XW, Ni S, et al. A tumor-targeted and conditionally replicating oncolytic adenovirus vector expressing TRAIL for treatment of liver metastases. *Mol Ther* 2004;9:496–509.
  46. Shinozaki K, Ebert O, Woo SL. Treatment of multifocal colorectal carcinoma metastatic to the liver of immune-competent and syngeneic rats by hepatic artery infusion of oncolytic vesicular stomatitis virus. *Int J Cancer* 2005;114:659–64.
  47. Solly SK, Trajceviski S, Frisen C, et al. Replicative retroviral vectors for cancer gene therapy. *Cancer Gene Ther* 2003;10:30–9.